



Small-angle neutron scattering study of coercivity enhancement in grain-boundary-diffused Nd–Fe–B sintered magnets



ABSTRACT

Keywords:

Coercivity
Nd–Fe–B
Permanent magnets
Small-angle neutron scattering

Isotropic Nd–Fe–B-based sintered magnets, before and after a (Tb-doped) grain-boundary diffusion process, have been investigated by means of magnetic-field-dependent small-angle neutron scattering. Compared to the untreated sample, we found a reduced correlation length in the grain boundary diffused sample which, in an applied-field range of 8.5 T, varies between 30 and 35 nm – about 15% smaller than in the untreated specimen. This observation is related to the increased magnetic anisotropy field of the nucleation sites for magnetization reversal, and may be explained by a reduction in the effective defect size responsible for the magnetic inhomogeneities.

© 2016 Elsevier B.V. All rights reserved.

1. Introduction

The discovery of Nd–Fe–B-based sintered magnets about three decades ago has triggered a remarkable development of new technologies, which comprise data transmission and recording, clean-energy generation, and transportation [1]. Despite this success, the limited intrinsic coercivity H_c of ternary Nd–Fe–B alloys at room temperature, combined with the substantial H_c drop at $T > 300$ K, still constitute the main bottlenecks for a wider usage of this engineering-relevant hard magnetic material.

To tackle this problem, different approaches have been pursued such as a reduction of the average grain size of the hard magnetic phase or the addition of alloying elements [2–4]. The latter is seen as a particularly promising approach in view of its straightforward industrial and laboratorial implementation. The so-called grain-boundary diffusion process (GBDP) has recently been employed to improve the magnetic hardness. In the GBDP, the Nd–Fe–B magnet is exposed at elevated temperatures to a fine powder or a vapor containing high-magnetic-anisotropy-inducing heavy-rare-earth elements such as Tb or Dy, which then diffuse (preferentially along liquid grain boundaries) into the bulk of the material, locally increasing the H_c [5–8]. In general, the results reported in Refs. [5–8] address both the material's microstructure as well as their magnetic properties after the GBDP. As an example, Sepehri-Amin et al. [9] employed electron microscopy, electron-probe microanalysis and three-dimensional atom-probe tomography to study the mechanism of H_c enhancement by the GBDP of Nd–Fe–B magnets. These authors report (as a consequence of GBDP using Dy vapor and subsequent heat treatment) the formation of both a Dy-rich shell and a Nd-rich grain-boundary phase layer in the outer region of the Nd₂Fe₁₄B grains. Despite the level of microstructural knowledge achieved so far, information about the effects of the GBDP on the *magnetic microstructure* of the

magnet *in the bulk* is still limited in the literature.

In this work, we employ the technique of small-angle neutron scattering (SANS) to investigate the influence of the GBDP on the magnetization-reversal process of Nd–Fe–B-based sintered magnets. SANS allows us to obtain information from within the volume of the magnet and on a mesoscopic length scale of about 1–300 nm (see, e.g., Refs. [10–12]).

2. Experimental

Isotropic Nd–Fe–B-based sintered magnets have been chosen for this study, since their spin-misalignment scattering (see below) is more pronounced than that of textured samples [13], allowing a more straightforward analysis and interpretation of real-space correlations. Two samples were investigated: as-received (AR, previously characterized and studied by means of SANS at QUOKKA instrument, ANSTO, Australia [14,15]) and after the GBDP (GBDP, Tb-doped, following the procedure described in Ref. [16]). The SANS experiment on the GBDP sample was carried out at 295 K at the instrument D33 at the Institute Laue-Langevin (ILL), Grenoble, France. A square-shaped sample with a side length of 15 mm and a thickness of about 630 microns was employed in the neutron experiment (magnetometric demagnetizing factor: $N \sim 0.052$ [17]). Unpolarized incident neutrons with a mean wavelength of $\lambda = 4.6$ Å and a wavelength spread of $\Delta\lambda/\lambda = 10\%$ (full width at half-maximum) were selected by means of a velocity selector. An external magnetic field \mathbf{H}_0 was applied perpendicular to the incident neutron beam direction. The SANS measurements were performed by first applying a large positive field (+6.9 T), which is assumed to bring the Nd–Fe–B sample into the major hysteresis loop (approach-to-saturation regime), and then reducing the field to the experimentally selected values following the magnetization curve. Neutron data were corrected for background scattering,

transmission, and detector efficiency using the GRASP software package [18]. The neutron transmission of both samples was larger than 90% at all fields. Magnetic characterization was performed on a needle-shaped sample ($1 \times 1 \times 7 \text{ mm}^3$) using a vibrating-sample magnetometer ($\mu_0 H_{\text{max}} = 10 \text{ T}$).

3. Results and discussion

Fig. 1 depicts the normalized magnetic hysteresis loops (at room temperature) of the AR and GBDP parts. Both magnetization curves exhibit a similar shape which is reminiscent of randomly-oriented noninteracting Stoner-Wohlfarth particles [19]. At 10 T, the remanence-to-polarization ratio equals ~ 0.5 , and the field at which the transition reversible \rightarrow irreversible magnetization takes place is at $\sim 3 \text{ T}$. The major difference between both specimens relates (as expected) to the optimization of H_c which increases by $\sim 16\%$ after the GBDP from 1.38 T (AR) to 1.60 T (GBDP). The observed improvement in H_c of the isotropic magnet studied in this work has the same order of magnitude as that previously reported for a textured magnet ($\sim 25\%$ [16]).

Fig. 2 compares the SANS results for the untreated (AR) and the GBDP sample. For the discussion of the data, it is useful to introduce the unpolarized SANS cross section, which, for the scattering geometry that has the applied magnetic field ($\mathbf{H}_0 \parallel \mathbf{e}_z$) perpendicular to the incoming neutron beam (parallel to the x -direction of a Cartesian laboratory coordinate system) reads [12]:

$$\frac{d\Sigma}{d\Omega}(\mathbf{q}) = \frac{8\pi^3 b_H^2}{V} \left[\frac{|\tilde{N}|^2}{b_H^2} + |\tilde{M}_x|^2 + |\tilde{M}_y|^2 \cos^2 \theta + |\tilde{M}_z|^2 \sin^2 \theta - (\tilde{M}_y \tilde{M}_z^* + \tilde{M}_y^* \tilde{M}_z) \sin \theta \cos \theta \right], \quad (1)$$

where V is the scattering volume, $b_H = 2.91 \times 10^8 \text{ A}^{-1} \text{ m}^{-1}$, $\tilde{N}(\mathbf{q})$ denotes the nuclear scattering amplitude, $\tilde{M}_{x,y,z}(\mathbf{q})$ represent the Fourier components of the magnetization vector field $M_{x,y,z}(\mathbf{r})$, the symbol “*” indicates the complex-conjugated quantity, and $\mathbf{q} \equiv (0, q_y, q_z) = q(0, \sin\theta, \cos\theta)$.

At the largest fields, both samples are on the major hysteresis branch in the approach-to-saturation regime (compare Fig. 1), and the two-dimensional SANS cross section (Fig. 2(a)) is elongated in the direction perpendicular to the field (which defines the

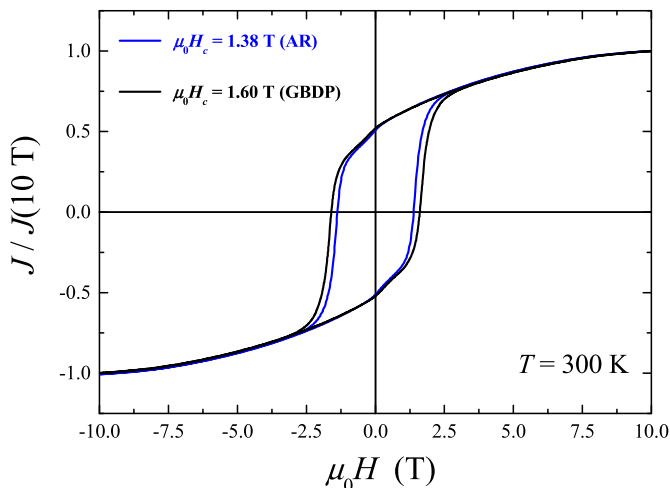


Fig. 1. Normalized room-temperature hysteresis loops of the isotropic Nd-Fe-B sintered magnets before (AR) and after the GBDP (see inset).

direction of the mean magnetization), in agreement with the term $\propto |\tilde{M}_z|^2 \sin^2 \theta$ in the cross section, Eq. (1); this effect is less pronounced (but present) in the GBDP sample at 6.9 T, which was the maximum field available in the ILL experiment. The field reduction results in the emergence of long-range, transversal, spin-misalignment fluctuations, which cause an angular anisotropy (related to the transversal magnetization Fourier components \tilde{M}_x and \tilde{M}_y in Eq. (1)) that is elongated in the direction parallel (and antiparallel) to the applied field. The spike-type “flying saucer” pattern with sharp maxima parallel to \mathbf{H}_0 , which starts forming at around 6 T in both samples, has been analyzed previously [15]; it is related to the formation of flux-closure patterns on a real-space length scale of the order of a few tens of nanometers.

The azimuthally-averaged 1D data (Fig. 2(b)) reveal for both samples a weak field dependence with a power-law-type behavior. Comparing intensities at the respective maximum field with H_c , the scattering signal at the smallest q changes by a factor of 3.2 (AR) and 3 (GBDP). For the GBDP sample, the $d\Sigma/d\Omega$ (nuclear and magnetic) can be overall well described by a q^{-4} decay, which is in agreement with exponentially correlated magnetization fluctuations [20]. The characteristic real-space length scale that is contained in the data appears to be weakly field dependent (see Fig. 3 below). As shown in Fig. 7 in Ref. [14], the $d\Sigma/d\Omega$ of the AR sample (after subtracting the scattering near saturation) is characterized by a weakly field-dependent power-law exponent n that is larger than 4, which is in agreement with the notion of spin-misalignment scattering, i.e., scattering due to transversally-misalignment spins with a characteristic magnetic-field-dependent wavelength [21]. The same statement applies to the GBDP sample (data not shown). We would also like to emphasize that the altered grain-boundary regions of the GBDP sample may (in addition to the magnetic scattering) have an impact on the nuclear SANS signal as well. This has been demonstrated for ensembles of polydisperse particles with a diffusive surface [22–24].

To estimate the length scale of the structural and magnetic correlations in both samples, we computed the correlation functions (see Ref. [14] and the inset in Fig. 3) from the total nuclear and magnetic $d\Sigma/d\Omega$ and determined the field dependency of the $(1/e)$ correlation length l_c (Fig. 3). The quantity l_c is (at a given field) a measure for the size of the inhomogeneously magnetized regions around microstructural defects such as the intergranular grain-boundary layers in Nd-Fe-B sintered magnets. We see in Fig. 3 that all the l_c values of the GBDP sample are smaller (between ~ 30 and 35 nm) than the ones of the untreated sample (~ 35 – 40 nm). The roughly 15% reduction in l_c seen in Fig. 3 may correspond to the observed 16% increase in H_c (Fig. 1).

It is well known that the GBDP results in a chemical composition gradient of the diffusing element. A previous study [16] using the same processing conditions as in the present work reports that the “penetration depth” on both sides of the sample is, respectively, larger than 200 microns. This finding then suggests that the neutron data that are taken from the present GBDP sample with a thickness of 630 microns represents a reasonable average between the Tb-lean and the Tb-rich parts of the specimen.

The l_c reduction may be a consequence of the formation of Tb-rich grain-boundary layers with a larger local coercivity as compared to the bulk of the grains, as discussed e.g. by Sepehri-Amin et al. [9]. In other words, as a consequence of the Tb-enrichment, the characteristic anisotropy field of possible nucleation sites for reversed domains such as grain boundaries is increased, which then yields an overall larger coercivity (see Fig. 1). In agreement with this assessment, the application of the Stoner-Wohlfarth model (for details the reader is referred to Ref. [25]) results in anisotropy fields of 7.7 T and 8.4 T for the AR and the GBDP specimens, respectively. The increased overall

Download English Version:

<https://daneshyari.com/en/article/1605889>

Download Persian Version:

<https://daneshyari.com/article/1605889>

[Daneshyari.com](https://daneshyari.com)